Proceedings of the XI DINAME, 28th February-4th March, 2005 - Ouro Preto - MG - Brazil
Edited by D.A. Rade and V. Steffen Jr.

TRANSIENT STABILITY OF EMPTY AND FLUID-FILLED CILINDRICAL SHELLS

Paulo Batista Gonçalves
Pontifical University of Rio de Janeiro - PUC - Rio, Civil Engineering Department. 22453-900 - Rio de Janeiro, RJ, Brazil.
paulo@civ.puc-rio.br

Zenon J. G. Nuñez del Prado
Federal University of Goiás, Civil Engineering Department. Praça Universitaria, 74605-200 -Goiânia, GO, Brazil.
zenon@eec.ufg.br

Frederico Martins Alves da Silva
Pontifical University of Rio de Janeiro - PUC - Rio, Civil Engineering Department. 22453-900 - Rio de Janeiro, RJ, Brazil.
fred0506@civ.puc-rio.br

Abstract. *In this work a qualitatively accurate low dimensional model is used to study the non-linear dynamic behavior of shallow cylindrical shell under axial loading. The dynamic version of the Donnell non-linear equations is solved by the Galerkin method. The shell is considered to be initially at rest in a potential well corresponding to a pre-buckling configuration. Then harmonic excitation is applied and conditions for escape from this potential well are sought. By defining steady state and transient stability boundaries, frequency regimes of instability may be identified such that they may be avoided in design. Initially a steady state analysis is performed; resonance response curves in the forcing plane are presented and the main instabilities are identified. Secondly, we investigate the global transient response of the system in order to quantify the degree of safety of the shell in the presence of small perturbations. Since the initial conditions, or even the shell parameters, may vary widely, and indeed are often unknown, attention is given to all possible transient motions. As parameters are varied, transient basins of attraction can undergo quantitative and qualitative changes; hence a stability analysis which solely considers the steady-state and neglects this global transient behavior, may be seriously non-conservative.*

Keywords: *cylindrical shells, fluid-structure interaction, parametric instability.*

1. Introduction

Thin-walled cylindrical shells are widely used in many industries. Due to increasing use of high-strength materials, sophisticated numerical techniques end optimization methods in analysis, the design of such shells is often buckling-critical. In many circumstances these shells are subjected not only to static loads but also to dynamic disturbances and filled with internal fluid. However, thin-walled cylindrical shells when subjected to axial compressive loads often exhibit a highly nonlinear behavior with a high imperfection sensitivity and may loose stability at loads levels as low as a fraction of the material's strength.

Many studies are concerned with the analysis of shells vibrating in vacuum; far fewer are focused on the analysis of the nonlinear vibrations of cylindrical shells in contact with a dense fluid. One of the first studies on vibrations of circular cylindrical shells in contact with a dense fluid considering shell nonlinearity is due to Ramachandran (1979). He studied the large-amplitude vibrations of circular cylindrical shells having circumferentially varying thickness and immersed in a quiescent, inviscid and incompressible fluid using the Donnell's shell theory.

Boyarshina (1984, 1988) studied theoretically the nonlinear free and forced vibrations and stability of a circular cylindrical tank partially filled with a liquid and having a free surface. Here, nonlinearity is attributed to the interaction of free surface waves and elastic flexural vibrations of the shell.

Gonçalves and Batista (1988) considered simply supported circular cylindrical shells filled with incompressible fluid. To model the shell, Sanders nonlinear shell theory and a novel mode expansion that includes two terms in the radial direction (the asymmetric and the axisymmetric ones) and ten terms to describe the in-plane displacements were used. Numerical results were obtained concerning the effect of the liquid on the nonlinear behavior of shells. It was found that the presence of a dense fluid increases the softening characteristics of the frequency-amplitude relation when compared with the results for the same shell in vacuo.

Chiba (1993) studied experimentally large-amplitude vibrations of two vertical cantilevered circular cylindrical shells made of polyester sheets partially filled with water to different levels. He observed that for bulging modes with the same axial wave number, the weakest degree of softening nonlinearity can be attributed to the mode having the minimum natural frequency, as observed for the same empty shells. He also found that shorter tanks have a larger softening nonlinearity than taller ones, as in vacuo. The tank with a lower liquid height has a stronger softening nonlinearity than the same tank with a higher liquid level. Traveling wave modes and coupling between two bulging modes (and between two sloshing modes) were also observed.

Amabili et al (1998) studied the nonlinear free and forced vibrations of a simply supported, circular cylindrical shell in contact with an incompressible and inviscid, quiescent dense fluid. Donnell's nonlinear shallow-shell theory is used, so that moderately large vibrations can be analyzed. The boundary conditions on radial displacement and continuity of circumferential displacement are exactly satisfied, while the axial constraint is satisfied "on the average". The problem is reduced to a system of ordinary differential equations by means of the Galerkin method, assuming an appropriate deflection shape. The mode shape is expanded by using two asymmetric modes (driven and companion modes) plus the axisymmetric mode.

In the present study, a low dimensional model which retains the essential nonlinear terms is used to study the nonlinear oscillations and instabilities of the shell. Here the interest is focused on a pivotal interaction between non-symmetric and axi-symmetric modes which produces escape from the pre-buckling potential well. To discretiza the shell, Donnell shallow shell equations, modified with the transverse inertia force, are used together with Galerkin method to derive a set of coupled ordinary differential equations of motion which are, in turn, solved by the Runge-Kutta method. In order to study the nonlinear behavior of the shell, several numerical strategies were used to obtain time response, Poincaré maps and bifurcation diagrams.

The fluid is modeled as non-viscous and incompressible and its motion is assumed to be irrotational. As a result, it can be characterized by a velocity potencial. The solution for the velocity potencial is taken as a sum of suitable functions, the unknown parameters of which are determined by the kinetic condition along the wetted surface of the shell (Batista and Gonçalves, 1988).

Steady state and transient stability boundaries are presented in which special attention is devoted to the determination of the critical load conditions. From this theoretical analysis, dynamic buckling criteria can be property established which may constitute a consistent and rational basis for design of these shell structures under harmonic loading.

2. Problem Formulation

2.1. Shell equations

Consider a perfect thin-walled fluid-filled circular cylindrical shell of radius R, length L, and thickness h. The shell is assumed to be made of an elastic, homogeneous, and isotropic material with Young's modulus E, Poisson ratio ν, and mass per unit area M. The axial, circumferential and radial co-ordinates are denoted by, respectively, x, y and z, and the corresponding displacements on the shell surface are in turn denoted by U, V, and W, as shown in Fig. 1.

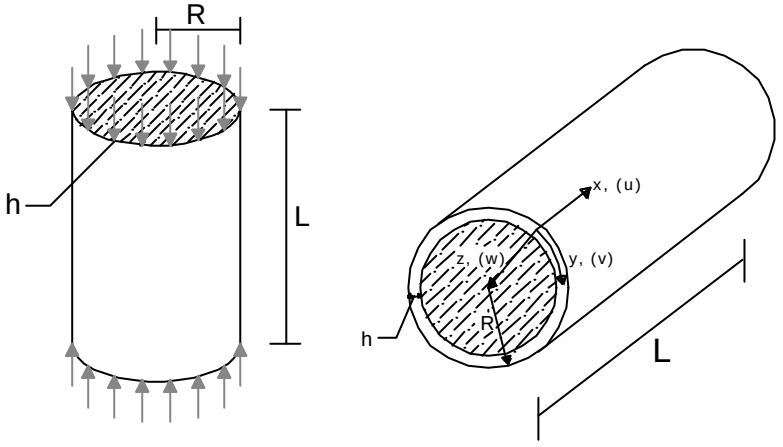

Figure 1. Shell geometry and coordinate system

The shell is subjected to a uniformly distributed axial load of the form:

$$P(t) = P_o + P_1 \cos(w\, t) \tag{1}$$

where P_o is the uniform static load applied along the edges x=0, L, P_1 is the magnitude of the harmonic load, t is time and ω is the forcing frequency.

The nonlinear equations of motion based on the Von Karmán-Donnell shallow shell theory, in terms of a stress function f and the transversal displacement w are given by:

$$M\ \ddot{w} + b_1\dot{w} + b_2\nabla^4\dot{w} + D\nabla^4 w = p_h R + F_{,yy}\ w_{,xx} + F_{,xx}\left(w_{,yy} + \frac{1}{R}\right) - 2F_{,xy}\ w_{,xy} \tag{2}$$

$$\frac{1}{Eh}\nabla^4 f = -\frac{1}{R} w_{,xx} - w_{,xx} w_{,yy} + w_{,xy}^2 \tag{3}$$

where

$$F = f^F + f \qquad f^F = -\frac{1}{2} P_0 y^2$$

and p_h is the fluid pressure, ∇^4 is the biharmonic operator, b_1 and b_2 are damping coefficients and D is the flexural rigidity defined as

$$D = E h^3 / 12\left(1 - n^2\right) \tag{4}$$

In the foregoing, the following non-dimensional parameters have been introduced:

$$W = \frac{w}{h} \qquad V = \frac{x}{L} \qquad q = \frac{y}{R} \qquad t = w_o\, t \qquad \Omega = \frac{w}{w_o}$$
$$\bar{f} = \frac{R}{E h^2 L^2} f \quad \Gamma_o = \frac{P_0}{P_{cr}} = \frac{R\sqrt{3\left(1-n^2\right)}}{E h^2} P_o \qquad \Gamma_1 = \frac{P_1}{P_{cr}} = \frac{R\sqrt{3\left(1-n^2\right)}}{E h^2} P_1 \tag{5}$$

Here ω_o is the lowest natural frequency of the empty shell.

2.2. Modal Analysis

The numerical model is developed by expanding the transversal displacement component w in series in the circumferential and axial variables. From previous investigations on modal solutions for the non-linear analysis of cylindrical shells under axial loads (Hunt et al. 1986; Gonçalves and Batista, 1988; Gonçalves and Del Prado, 2002) it is observed that, in order to obtain a consistent modeling with a limited number of modes, the sum of shape functions for the displacements must express the non-linear coupling between the modes and describe consistently the unstable post-buckling response of the shell as well the correct frequency-amplitude relation.

The lateral deflection w can be generally described as (Gonçalves and Batista, 1988):

$$W = \sum_{i=1,3,5} \sum_{j=1,3,5} W_{ij} \cos\left(i\, nq\right) sin\left(j\, mp\, V\right) + \sum_{k=0,2,4} \sum_{l=0,2,4} W_{ij} \cos\left(k\, nq\right) sin\left(l\, mp\, V\right) \tag{6}$$

where n is the number of waves in the circumferential direction of the basic buckling or vibration mode, m is the number of half-waves in the axial direction, $q = y/R$ and $V = x/L$.

These modes represent both the symmetric and asymmetric components of the shell deflection pattern. The first double series represents the unsymmetrical modes with odd multiples of the basic wave numbers m and n. The second double series represents, besides the asymmetric modes which contains an even multiple of the basic wave numbers m and n and rosette modes, the axy-simmetric modes which play an important role in the non-linear modal coupling and loss of stability of the shell.

Previous studies on buckling of cylindrical shells have shown that the most important modes are the basic buckling or vibration mode and the axi-symmetric mode with twice the number of half waves in the axial direction as the basic mode, that is:

$$W = z\left(t\right)_{11} \cos\left(nq\right) \mathrm{sen}\left(mp\, V\right) + z\left(t\right)_{02} \cos\left(2mp\, V\right) \tag{7}$$

The relevance of these modes from a physical point of view is explained by Croll and Batista (1981) and from symmetry and catastrophe theory arguments by Hunt et al. (1986). Thes modes are enough to describe the initial post-buckling behavior of the shell as well as the topology of the pre-buckling well and the potential barrier connected with the unstable equilibrium positions lying on the initial post-buckling path.

Substituting the assumed form of the lateral deflection, Eq. (7), on the right-hand side of the compatibility Eq. (3) one can solve it for the stress function f in terms of w together with the relevant boundary and continuity conditions. Upon substituting the modal expressions for f and w into Eq. (2) and applying the Galerkin method, a set of non-linear ordinary differential equations is obtained in terms of modal amplitudes $\zeta(\tau)_{ij}$.

2.3 Fluid Equations

The shell is assumed to be completely fluid-filled. The irrotational motion of an incompressible and non-viscous fluid can be described by a velocity potential $f(x,r,q,t)$. This potential function must satisfy the Laplace equation which can be written in dimensionless form as:

$$\bar{f}_{,W} + \frac{1}{k}\bar{f}_{,k} + \frac{1}{k^2}\bar{f}_{,qq} + \bar{f}_{,kk} = 0 \tag{8}$$

where $k = r/R$ and $\bar{f} = g\,f/R^2$.

The influence of the nonlinearities in the fluid formulation is very small so that the fluid can be considered as linear. Therefore the hidrodynamic fluid pressure can be written as:

$$p_h = z_{11,tt}\; m_a \cos(nq)\sin(mp\,x) \tag{9}$$

where m_a is the added mass due to the fluid contained in shell, which is given by:

$$m_a = (r_F\,R)\left\{mp\,x\left[\frac{I_{n-1}(mp\,V)}{I_n(mp\,V)} - \frac{n}{mp\,V}\right]\right\}^{-1} \tag{10}$$

Here ρ_F is the density of the fluid, ρ_S is the shell material density and I_{n-1} and I_n are Bessel functions.

3. Results.

Consider a thin-walled cylindrical shell with h=0,002 m, R=0,2 m, L=0,4 m, E=2,1x10^8 kN/m2, ν=0,3, M=78,5 kg/m^2, $\beta_1=2\varepsilon M\omega_0$, with ε=0,003 (fluid-filled shell) and ε=0,0008 (empty shell), and $\beta_2=\eta D$ with η=0,0001. The shell and fluid densities are: ρ_s=7850 kg/m^3 and ρ_F=1000 kg/m^3. For this shell geometry the lowest natural frequency occurs for *(n,m)=(5,1)*.

Now the parametric instability and escape of the fluid-filled cylinder under axial harmonic forcing, as described by Eq. (1), will be considered. In the following, the constant part to the loading Γ_0 is assumed to lie between the upper and lower static critical load of the shell. In these circumstances, the shell potential energy exhibits three wells, one associated with the fundamental pre-buckling configuration and two wells associated with the two possible post-buckling configurations. If the cylinder is subjected to a periodic axial load, it will undergo the familiar longitudinal forced vibration, exhibiting a uniform transversal motion, due to the effect of Poisson's ratio, also known as breathing mode. However, at certain critical values, the longitudinal motion becomes unstable and the cylinder executes transverse bending vibrations. Figure 2 shows some representative time histories for Γ_0=0,80. Here $\Omega = w/w_o$ and w_o is the lowest natural frequency of the unloaded shell. A projection of the phase space and Poincaré section are also shown in these figures. These figures were obtained by numerically integrating the equation of motion through the Runge-Kutta integration scheme. In Fig. 2.a, for a forcing amplitude lower than a critical value (Γ_1=0,28 and Ω = 0,80), after a finite initial disturbance, the amplitude of the response decreases rapidly converging to the trivial solution. If the control parameter Γ_1 is increased beyond a critical value, the shell exhibits initially an exponential growth of the amplitude, as shown in Fig. 2.b, converging to a limit cycle within the pre-buckling well. In this case, the trivial solution becomes unstable (parametric instability) and the system converges to a period-two stable solution. If, Γ_1 is increased to a higher value, for example Γ_1 = 0,50, the shell escapes from the pre-buckling well (snap-through buckling) and exhibits large cross-well chaotic motions, as shown in Fig. 2.c, or small amplitude oscillation around a post-buckling configuration.

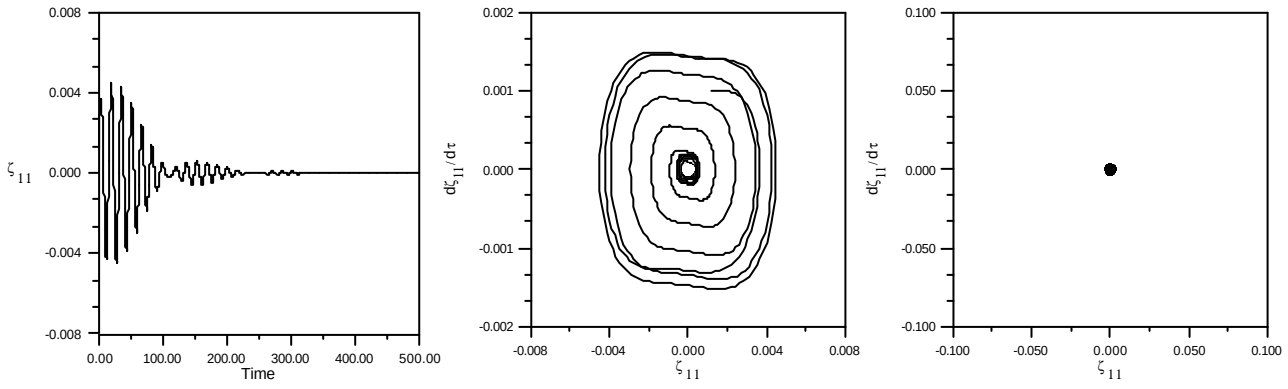

(a) Γ_1 = 0,28

Figure 2 – Continues in the following pagina.

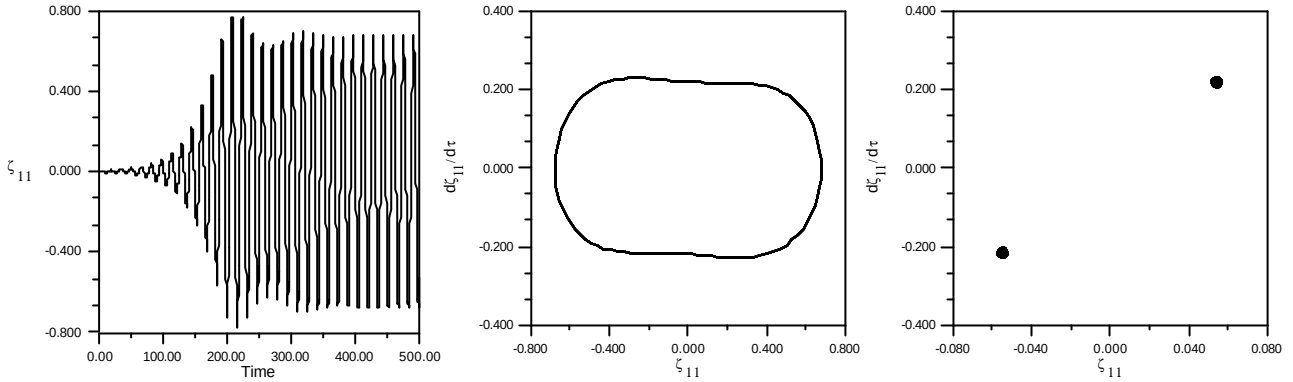

(b) $\Gamma_1 = 0{,}32$

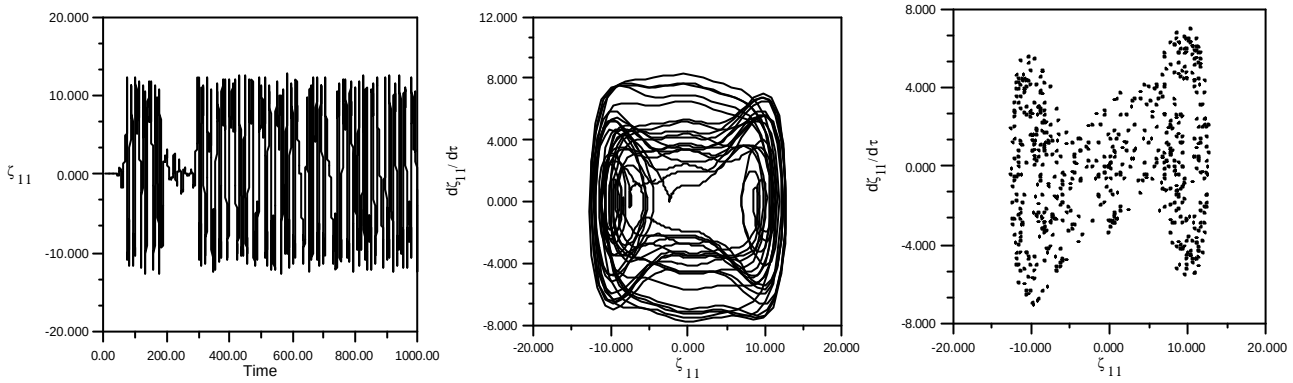

(d) $\Gamma_1 = 0{,}50$

Figure 2. Time response, phase plane and Poincaré section for $\Gamma_o = 0{,}80$ and $\Omega = 0{,}80$. Fluid-filled circular cylindrical shell.

Figure 3 shows the numerically obtained parametric instability boundary as well as the transient and permanent escape boundaries for fluid-filled shell and the same shell in *vacuo*, in (frequency of excitation, amplitude of excitation) control space for Γ_o=0,80, Γ_o=0,60 and Γ_o=0,40. The lower stability boundary corresponds to parameter values for which small perturbations from the trivial solution will result in an initial growth in the oscillations; therefore it defines the parametric instability boundary. The second limit corresponds to escape from the pre-buckling potential well in a slowly evolving environment. These curves were obtained by increasing slowly the amplitude while holding the frequency constant. As one can observe, the parametric stability boundary is composed of various "curves", each one associated with a particular bifurcation event. The deepest well is associated with the principal instability region at $w=2w_p$, while the second well to the left is the secondary instability region occurring around $w=w_p$ and the other smaller wells to the left are connected with super-harmonic resonances. The horizontal dotted line corresponds to the static critical load of this shell. Comparing Figures 3.a, 3.b and 3.c, one can conclude that the static pre-loading has the effect of lowering the stability boundaries, of enlarging the width of the instability regions and of shifting the instability regions to the left. In both cases the instability boundaries can be much lower than the static critical load. The fluid has a similar influence on the stability boundaries. This is expected since the influence of the fluid is to increase the effective mass of the system, decreasing consequently the natural frequencies.

For the region between the parametric instability limit and the transient escape limit, the shell exhibits vibrations in the pre-buckling potential well during both permanent and transient states. When comparing the permanent and transient boundaries, one can observe that the transient escape limit is lower than the permanent escape limit. This means that the shell may exhibit large amplitude vibrations during the transient state but converge to a low amplitude solution within the pre-buckling well when the steady-state response in reached. It must be pointed out that a structure may display in a nonlinear regime long transients, the length of which can not be known *a priori*. So, in order to avoid any damage due to large amplitude vibrations the transient response of the shell must be analyzed in detail.

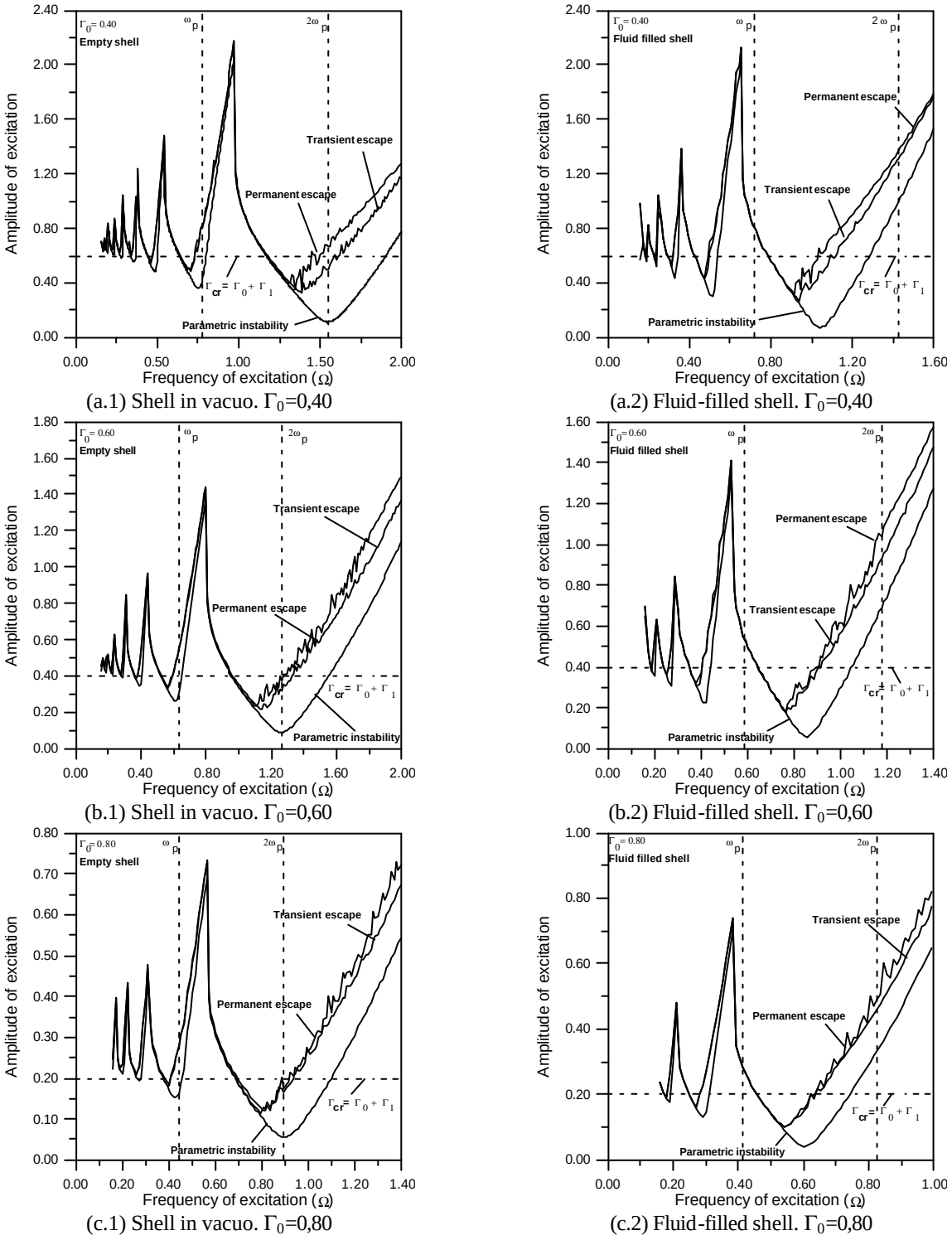

Figure 3. Instability boundaries in control space for different values of static load.

Figure 4 shows typical bifurcation diagrams connected with the principal instability region for the fluid-filled shell as a function of the forcing amplitude Γ_1, for different values of the forcing frequency Ω. These bifurcation diagrams where obtained by numerical continuation techniques. In these diagrams a dotted line means unstable solutions and a continuous line means stable solutions. The bifurcation diagram depicted in Fig. 4.a is typical of the left, descending branch of the principal region of parametric instability. The system exhibits a sub-critical bifurcation, that is, the fundamental solution looses its stability, giving rise to a 2T unstable periodic motion. In this case, any increase in Γ_1 beyond the critical value leads to a jump to another stable solution that may exist within the pre-buckling well or around a post-buckling configuration. Also, the 2T solution exhibits a stable branch between two unstable branches. So, for load levels lower than the critical value the shell may display different types of behavior within the pre-buckling well. As observed in Fig. 4.a, this non-trivial stable region corresponds to forcing values lower than the critical load. This leaves a regime where there is no attractor within the pre-buckling well after the critical point is reached and hence an

inevitable jump to escape under increasing forcing occurs. This explains why in this region the numerically obtained parametric instability boundary practically coincides with the transient and permanent escape boundaries.

In Fig. 4.b, the jump is indeterminate. The bifurcation is sub-critical, but the stable small-amplitude non-trivial solution subsists for forcing values higher than the critical load. So, when the fundamental trivial solution becomes unstable, the response may re-stabilize within the pre-buckling well or jump to a remote attractor. The response that is attained physically depends on the initial conditions.

The bifurcation diagram shown in Fig. 4.c is typical of the right, ascending branch of the stability boundary. When Γ_1 is lower than the critical value, the only possible steady state solution within the pre-buckling well is the trivial one, which is stable. Consequently, the response is trivial. When Γ_1 is greater than a critical value, there are two possible steady state solutions: (a) the trivial one, which is unstable; and (b) a finite amplitude period-two (2T) solution, which is stable. In this case, since disturbances are always present, the response is non-trivial. Also, these figures show that as Γ_1 increases from zero, the response consists of the trivial solution. As Γ_1 exceeds the critical value, ζ_{11} begins to increase slowly with increasing Γ_1. The critical value is in this case is a supercritical bifurcation. As the amplitude of the forcing increases, the amplitude of the response increases until the escape boundary is reached. Before escape occurs, the period-two solution may also become unstable, being followed by a period doubling cascade, eventually reaching a narrow zone of chaotic motion.

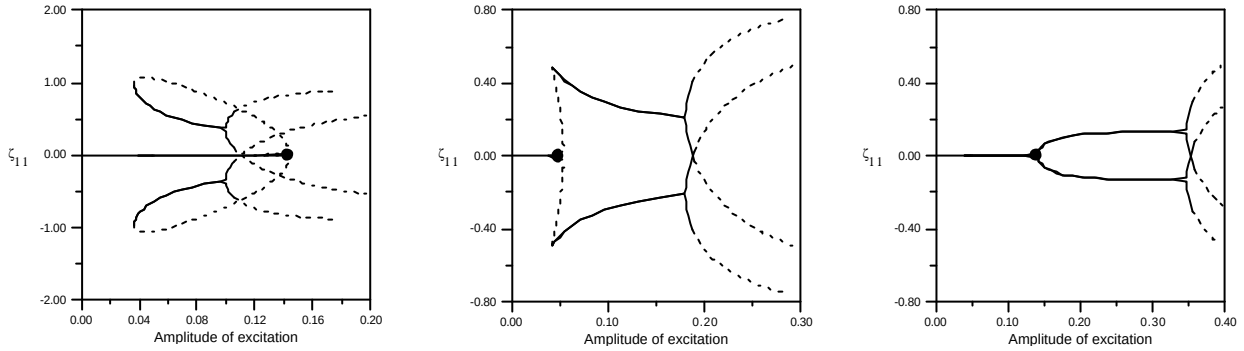

(a) Ω = 0,50 (b) Ω = 0,58 (c) Ω = 0,65

Figure 4. Bifurcation diagrams of the Poincaré map. Principal instability region for fluid-filled shell, Γ_0 = 0,80.

In order to evaluate the safety of the structure one should analyze the behavior of the basins of attraction of the solutions in both transient and permanent states. Figure 5 shows the evolution of the transient basin de attraction for increasing values of the forcing amplitude Γ_1, Ω = 0,65 and Γ_o=0,80. Here the $\zeta_{11} \times \zeta_{02}$ cross-sections of the four dimensional phase space $\left(\dot{z}_{11} = \dot{z}_{02} = 0{,}0\right)$ are shown for increasing values of the forcing amplitude. Figure 6 shows the evolution of the permanent basin de attraction for increasing values of the forcing amplitude Γ_1, Ω = 0,65 and Γ_o=0,80. Both figures are associated with the bifurcation diagram of Fig. 4.c and cover the same set of initial conditions.

In Fig. 5 the green area is associated to escape during the transient response and the white area corresponds to the fundamental trivial and period two stable solutions within the pre-buckling well. As Γ_1 increases the region associated with escape increases and after a certain critical value, it covers completely the analyzed region, showing that escape occurs for any set of initial conditions during the transient response well before the critical escape load displayed in the bifurcation diagram of Fig. 4.c.

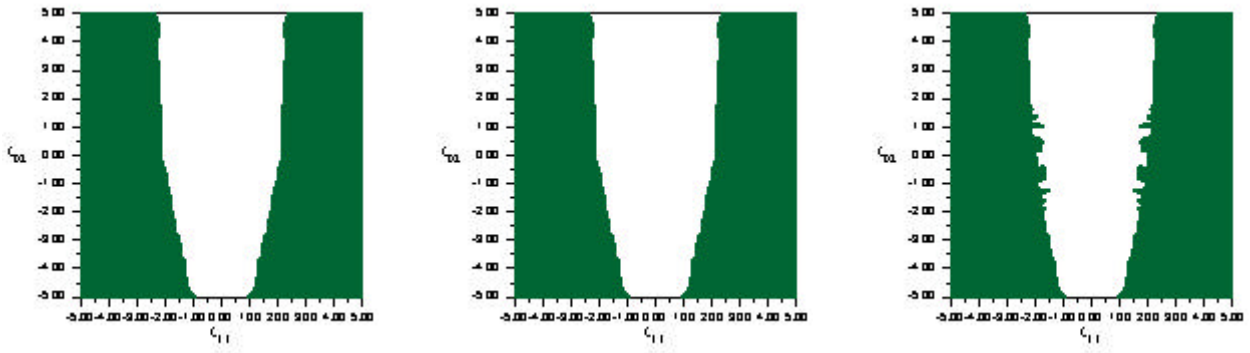

(a) Γ_1 =0,02 (b) Γ_1 =0,05 (c) Γ_1 =0,074

Figure 5 – Continues in the following pagina.

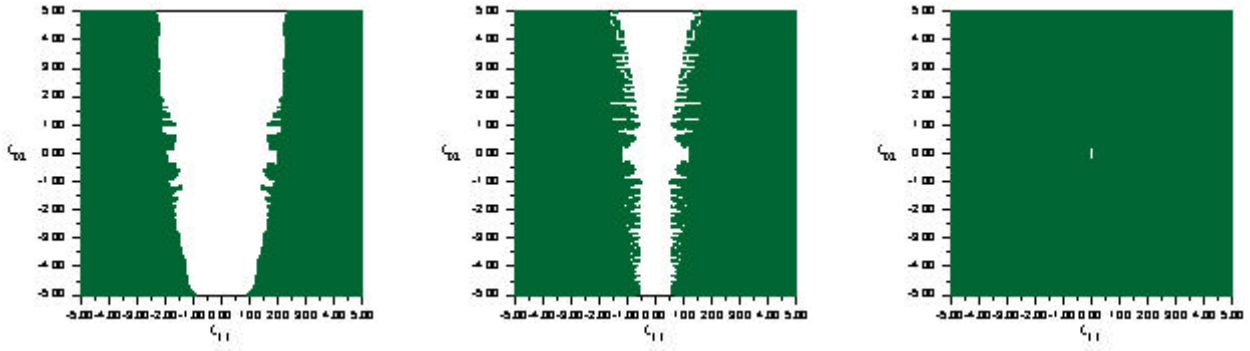

(d) Γ_1 =0,08 (e) Γ_1 =0,15 (f) Γ_1 =0,23

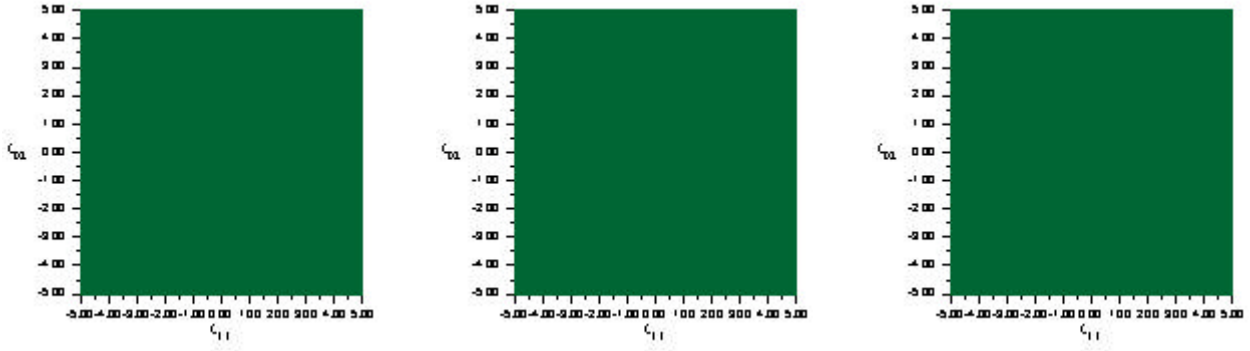

(g) Γ_1 =0,265 (h) Γ_1 =0,275 (i) Γ_1 =0,279

Figure 5. Projections of the basins of attraction, in transient state, for increasing values of the forcing amplitude Γ_1 of the fluid-filled cylindrical shell. Evolution of the basin for Γ_0 = 0,80 and Ω = 0,65. Parametric instability load = 0,076.

In. Fig. 6 the black area corresponds to the fundamental trivial solution, the read and blue areas correspond to the period two stable solution within the pre-buckling well and the white area corresponds to escape. For Γ_1 lower than the critical point, the response for initial conditions within the analyzed area converges to the trivial solution or to escape. Of course, escape can only occur for large perturbations. After the critical point, the black region suddenly disappears and the response for the majority of initial conditions converges to the period two stable solutions within the pre-buckling well. As Γ_1 increases, the region associated with this solution decreases and a rapid erosion is observed. Also, after a certain critical value the whole basin of attraction becomes fractal. In this case the response becomes very sensitive to the initial conditions and the steady state response, unpredictable.

Comparing the trivial and period two areas of Fig. 5 and Fig. 6, one can observe that the basin area occupied by the transient response is smaller than the area occupied by the permanent response. So, a practical design criterion must be based on the transient analysis rather than on the steady state response of the system. Also, the critical loads obtained from the bifurcation diagrams are not enough to evaluate the robustness of the structure in the presence of unavoidable disturbances occurring during its construction or service life. The analysis of size and structure of the basin of attraction must be taken into account in order to specify allowable disturbances in a dynamic environment. A detailed parametric analysis of the basin evolution considering empty and fluid-filled shells can be found in Silva (2004).

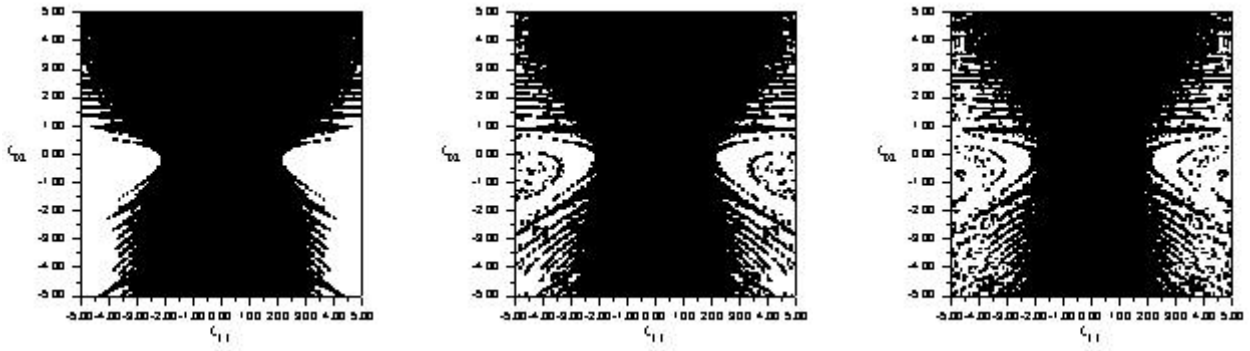

(a) Γ_1 =0,02 (b) Γ_1 =0,05 (c) Γ_1 =0,074

Figure 6 – Continues in the following pagina.

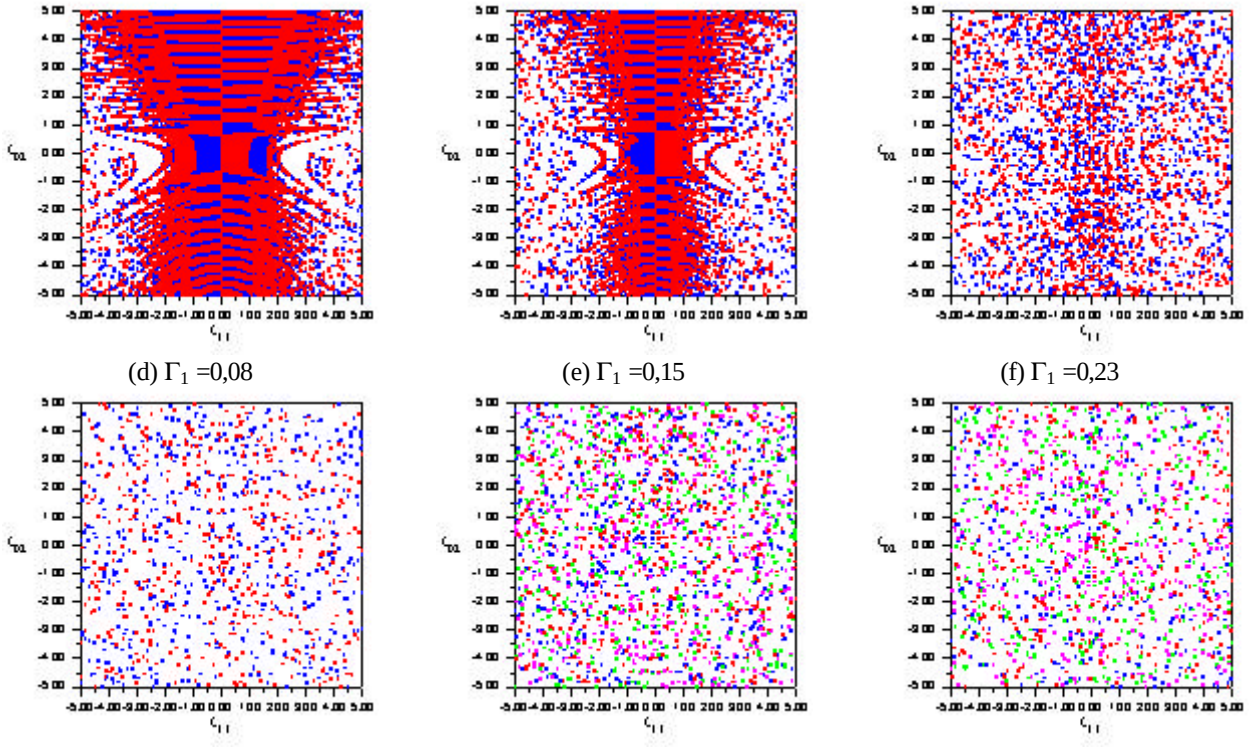

(d) Γ_1 =0,08 (e) Γ_1 =0,15 (f) Γ_1 =0,23

(g) Γ_1 =0,265 (h) Γ_1 =0,275 (i) Γ_1 =0,279

Figure 6. Projections of the basins of attraction, in permanent state, for increasing values of the forcing amplitude Γ_1 of the fluid-filled cylindrical shell. Evolution of the basin for Γ_0 = 0,80 and Ω = 0,65.
Parametric instability load = 0,076.

4. Concluding Remarks

Based on Donnell's shallow shell equations, an accurate low-dimensional model is derived and applied to the study of the nonlinear vibrations of an axially loaded fluid-filled circular cylindrical shell in transient and permanent states. The results show the influence of the modal coupling on the post-buckling response and on the nonlinear dynamic behavior of fluid-filled circular cylindrical shells. Also the influence of a static compressive loading on the dynamic characteristics is investigated with emphasis on the parametric instability and escape from the pre-buckling potential well. The most dangerous region in parameter space is obtained and the triggering mechanisms associated with the stability boundaries are identified. Also the evolution of transient and permanent basin boundaries is analyzed in detail and their importance in evaluating the degree of safety of a structural system is discussed. It is shown that critical bifurcation loads and permanent basins do not offer enough information for design. Only a detailed analysis of the transient response can lead to safe lower bounds of escape (dynamic buckling) loads in the design of fluid-filled cylindrical shells under axial time- dependent loads.

5. Acknowledgements

This work was made possible by the financial support in form of a research grant from the Brazilian Research Council – CNPq.

6. References

Amabili, M., Pellicano, F. & Païdoussiss, M., 1998, "Nonlinear Vibrations of Simply Supported Circular Cylindrical Shells, Coupled to Quiescente Fluid", Journal of Fluids and Structures, Vol. 12, pp. 883-918.

Amabili, M., Pellicano, F. and Païdoussis, M. P., 2000, "Nonlinear vibrations of fluid-filled, simply supported circular cylindrical shells: theory and experiments", Nonlinear Dynamics Plates and Shells; AMD, . New York: ASME, Vol. 238, pp. 73-84

Amabili, M., Pellicano, F. and Païdoussis, M. P., 2001, "Nonlinear supersonic flutter of circular cylindrical shells", AIAA J., Vol. 39, pp. 564-573.

Boyarshina, L. G., 1984, "Resonace effects in the nonlinear vibrations of cylindrical shells containing a liquid", Soviet Applied Mechanics, Vol. 20, pp. 765-770.

Boyarshina, L. G., 1988, "Nonlinear wave modes of an elastic cylindrical shell partially filled with a liquid under conditions of resonance", Soviet Applied Mechanics, Vol. 24, pp. 528-534.

Chiba, M., 1993, "Non-Linear Hydroelastic Vibration of a cantilever Cylindrical Tank", International Journal of Non-Linear Mechanics, Vol. 28, pp. 591-559.
Croll, J. G. A. and Batista, R. C., 1981, "Explicit Lower Bounds for the Buckling of Axially Loaded Cylinders", International Journal of Mechanical Science, Vol. 23, pp. 331-343.
Gonçalves, P. B. and Batista, R. C., 1988, "Non-Linear Vibration Analysis of Fluid-Filled Cylindrical Shells", Journal of Sound and Vibration, Vol. 127, pp. 133-143.
Gonçalves, P. B. and Del Prado, Z. J. G. N., 2000, "The Role of Modal Coupling on the Non-linear Response of Cylindrical Shells Subjected to Dynamic Axial Loads", In: Nonlinear Dynamics of Plates and Shells; AMD – Vol. 238, pp. 105-116. New York: ASME.
Gonçalves, P. B. and Del Prado, Z. J. G. N., 2002, "Non-Linear Oscillations and Stability of Parametrically Excited Cylindrical Shells", Meccanica, Vol. 37, pp.569-597.
Hunt, G. W., Williams, K. A. J. and Cowell, R. G., 1986, "Hidden Symmetry Concepts in the Elastic Buckling of Axially Loaded Cylinders", International Journal of Solid and Structures, Vol. 22, pp. 1501-1515.
Yamaki, N., 1984, "Elastic Stability of Circular Cylindrical Shells", Ed. Amsterdam: North Holland.
Ramachandran, J., 1979, "Nonlinear Vibrations of Cylindrical Shells of Varying Thickness in an Incompressible Fluid", Journal of Sound and Vibration, Vol. 64, pp: 97-106.
Silva, F. M. A. "Análise da Instabilidade Dinâmica de Cascas Cilíndricas com Fluido Interno". 2004. Dissertação de Mestrado, UFG-GO, Goiânia-GO, Brazil, 2004.

5. Responsibility notice

The authors Paulo Batista Gonçalves, Zenon. J. G. Nuñez del Prado and Frederico Martins A. da Silva are the only responsible for the printed material included in this paper.